Thermochimica Acta 399 (2003) 99–108

thermochimica acta

www.elsevier.com/locate/tca

Thermodynamics of crystalline dimer of fullerene C_{60} in the range from $T \rightarrow 0$ to 340 K at standard pressure

B.V. Lebedev [a,*], A.V. Markin [a], V.A. Davydov [b],
L.S. Kashevarova [b], A.V. Rakhmanina [b]

[a] *Chemistry Institute, Nizhny Novgorod State University, Gagarin Prospekt 23/5, 603950 Nizhny, Novgorod, Russia*
[b] *Institute for High Pressure Physics, Russian Academy of Sciences, 142190 Troitsk, Moscow, Russia*

Received 18 February 2002; received in revised form 26 July 2002; accepted 29 July 2002

Abstract

By adiabatic vacuum calorimetry the temperature dependence of heat capacity for crystalline dimer of fullerene C_{60} has been determined in the range 6–340 K at standard pressure. Between 46 and 56 K, a glass-like transition of the dimer, the nature of which is, probably, similar to that described for C_{60}, has been found. The results were used to calculate the thermodynamic functions of the dimer: the heat capacity $C_p^\circ(T)$, enthalpy $H^\circ(T) - H^\circ(0)$, entropy $S^\circ(T) - S^\circ(0)$ and Gibbs function $G^\circ(T) - H^\circ(0)$ over the range from $T \rightarrow 0$ to 340 K. For $T < 60$ K the fractal dimension D in the heat capacity function of the multifractal variant of the Debye's theory of heat capacity was estimated and in the 20–45 K range D was found to be 1. That indicates a chain structure of the dimer. The heat capacities of the dimer have been compared to those of the initial fullerite C_{60}. The standard entropy of formation of the crystalline dimer from graphite, at $T = 298.15$ K and at standard pressure, and the entropies of transition of the initial fullerite C_{60} to the crystalline dimer have been calculated.

Keywords: Monomeric fullerene C_{60}; Dimer $(C_{60})_2$; Heat capacity; Thermodynamic functions

---

1. Introduction

The transformations of fullerite C_{60} under high pressures and at elevated temperatures are accompanied by the formation of numerous high-pressure phases [1–9]. In the region of the stability of molecular cluster C_{60}, these phases are formed on the base of dimeric, low-molecular oligomeric and high-molecular one-dimensionally (1D), two-dimensionally (2D) and three-dimensionally (3D) polymerized C_{60}. When C_{60} is exposed to the treatment at temperatures above the stability limit of C_{60} cluster, many atomic carbon states are formed. A series of transformations is terminated with the formation of equilibrium phases—graphite and diamond. Products of T–P treatment of C_{60} can be kept under usual conditions in metastable but stable states for a long time. It follows from the research results that some metastable phases exhibit unique properties: superhardness [5–8], record crack resistance [7], ferromagnetism [10] and others [11,12]. It should be noted that a part of them has found already a wide application in practice, for example ultrahard fullerite is used in a scanning microprofilometer in which a needle for measuring hardness and a probe were manufactured from this fullerite [11,13].

In [14–19] the data on calorimetric measurements of some metastable phases, particularly, crystalline 1D

---

[*] Corresponding author. Fax: +7-8312656450.
E-mail address: lebedevb@ichem.unn.runnet.ru (B.V. Lebedev).

PII: S0040-6031(02)00450-1

and 2D polyfullerenes are cited. However, up-to-now the study of the thermodynamic properties of crystalline dimer was not carried out yet.

The aim of the present work is to determine the temperature dependence of the heat capacity for $(C_{60})_2$—crystalline dimer of fullerene C_{60}—in the range from $T \to 0$ to 340 K, to study possible physical transformations on heating and cooling and to calculate the thermodynamic functions $C_p^\circ(T)$, $H^\circ(T) - H^\circ(0)$, $S^\circ(T) - S^\circ(0)$, $G^\circ(T) - H^\circ(0)$ for the range of 0–340 K, and also to compare the heat capacities of $(C_{60})_2$ with the initial fullerite C_{60}, to determine fractal dimension D for $(C_{60})_2$ in the heat capacity function [20,21], to calculate the standard entropy of formation of the crystalline dimer (from graphite at 298.15 K) and the entropy of reaction $2C_{60}(cr) \to (C_{60})_2$ under the same physical conditions.

2. Experimental

2.1. Sample

Twice sublimated fine-dispersed crystalline powder of fullerite (99.98 mass% C_{60}), prepared by the Term Company, USA was used as initial material to synthesize dimeric $(C_{60})_2$. Samples were synthesized on a high-pressure device “Maxim” (piston—cylinder type) at 1.5 GPa and 423 K with a period of isothermal exposure of 1000 s. Dimerized states, formed by quenching under pressure and kept under normal conditions, were withdrawn from the high-pressure device and characterized by X-ray diffraction and oscillation spectroscopy. Diffractograms of powder-like samples were recorded on a INEL CPS 120 diffractometer by using Cu Kα1 irradiation. IR spectra of samples were recorded on a Specord M 80 (Carl Zeiss) spectrophotometer. Raman spectra were examined by means of a Bruker FT Raman RFS100 spectrometer. A X-ray diffractogram and oscillation spectra of the sample with the maximal content of the dimeric phase (ca. 80 mol% the dimer $(C_{60})_2$ and ca. 20 mol% the monomer C_{60}), taken for the subsequent calorimetric measurements, were described in detail earlier [9,22,23]. It is noted that some low-molecular polymerized C_{60} were available as traces in the sample and their indisputable identification was, unfortunately, unsuccessful.

The calorimetric measurements confirmed the composition of the examined sample (the content of the initial C_{60} that remained non-transformed to $(C_{60})_2$ in the process of high pressure–temperature treatment was determined to be 21 mol%). The sample of the dimerized state containing 79 mol% $(C_{60})_2$ and 21 mol% C_{60} was denoted DS and was studied in an adiabatic vacuum calorimeter. The properties of the mixture of $(C_{60})_2$ and C_{60} were supposed to be additive.

2.2. Apparatus and measurement procedure

An automated thermophysical device (BKT-3), an adiabatic vacuum calorimeter, was employed to measure the heat capacity. The design of the calorimeter and the procedure of the heat capacity measurements have been described earlier [24,25]. From the calibration and testing results of the calorimeter, it was found that the uncertainty of the heat capacity measurements at liquid helium temperatures is within to ±2%. As temperature rises up to 40 K, it decreases to ±0.5% and becomes approximately equal to ±0.2% between 40 and 340 K.

3. Results and discussion

3.1. Heat capacity

The heat capacity C_p° of the DS sample was measured in the 6–340 K range. The sample mass was 0.4044 g. The 271 experimental C_p° points were taken in five series (Table 1). The heat capacity of the sample itself was between 10 and 30% of the total heat capacity (calorimetric ampoule and sample). Averaging of the experimental C_p° values was performed by means of degree and semilogarithmic polynomials. The root mean square deviation of the C_p° values from the corresponding smoothed $C_p^\circ = f(T)$ curve was within ±0.5% in the range 6–80 K and ±0.04% between 80 and 340 K. The experimental values of C_p° and the averaged curve are shown in Fig. 1. For comparison, Fig. 1 also shows the heat capacity of the fullerite C_{60} [26]. It is seen that for DS a physical transition appears in the temperature interval from 185 to 280 K, as in the case of the fullerite C_{60}. However, judging by the ratio of the corresponding areas under the curves of

Table 1
Experimental values of heat capacity of sample DS (mixture of 79 mol% dimer $(C_{60})_2$ and 21 mol% C_{60}) per mole of C_{60}; $M = 720.66$ g/mol

T (K)	C_p° (J/(K mol))	T (K)	C_p° (J/(K mol))	T (K)	C_p° (J/(K mol))
Series 1		9.93	12.28	55.14	49.65
6.84	6.632	10.44	13.21	56.45	50.01
7.82	8.790	10.96	13.97	57.75	50.47
8.84	10.63	11.46	14.92	Series 4	
9.36	11.08	11.98	15.70	86.08	71.65
9.88	12.35	12.64	16.75	88.52	74.60
10.41	13.07	13.45	18.59	90.98	77.55
10.91	13.96	14.25	18.95	93.43	80.70
11.46	14.75	15.01	20.13	95.87	83.92
11.97	15.60	15.76	21.01	98.32	87.57
12.62	16.65	17.25	23.10	100.76	90.51
13.40	17.85	18.08	24.17	103.20	94.23
14.21	19.20	19.50	26.01	105.64	97.34
14.97	20.15	20.21	26.05	108.07	101.0
15.87	21.23	21.95	29.17	110.50	105.4
16.62	22.25	24.40	31.20	112.93	109.3
17.34	23.20	26.93	32.85	115.35	112.8
18.06	24.30	29.42	33.46	117.78	117.5
18.79	25.10	31.89	36.26	120.21	121.7
19.52	26.05	34.36	37.70	122.63	126.1
20.28	26.81	36.85	39.28	125.03	131.0
22.01	29.30	39.35	40.20	127.44	135.2
24.48	31.14	44.35	42.49	129.85	139.3
27.01	32.00	46.85	43.60	132.26	144.8
29.50	33.85	49.35	46.01	134.66	149.1
31.97	36.32	51.85	47.70	137.05	154.8
34.45	37.30	54.36	49.74	139.45	158.6
36.95	39.44	56.87	50.05	141.84	164.2
39.46	40.31	59.39	51.04	144.24	169.4
41.97	41.47	Series 3		146.62	174.8
44.47	42.60	20.31	27.24	149.01	179.6
46.96	43.96	23.03	30.03	151.39	185.3
49.46	45.89	25.81	32.00	153.77	190.5
51.96	47.95	27.19	33.10	156.14	196.2
54.47	49.22	28.56	33.99	158.51	201.5
56.99	50.44	29.92	35.02	160.88	206.7
62.04	51.46	31.29	36.01	163.21	212.4
64.55	52.77	32.64	36.75	165.57	217.7
67.06	54.07	33.98	37.52	167.93	222.7
69.58	55.85	35.33	38.30	170.28	229.3
72.10	57.60	36.67	39.11	172.62	235.0
74.62	59.50	39.33	40.26	174.96	239.9
77.14	61.80	41.99	41.52	177.30	246.5
79.67	64.25	43.37	42.10	179.64	252.0
82.18	67.10	44.68	42.72	181.96	261.1
84.70	70.10	45.99	43.30	186.56	269.7
Series 2		47.29	44.10	188.86	275.9
7.05	6.813	48.60	44.83	191.16	281.7
7.96	8.722	49.90	46.10	193.45	286.1
8.37	9.514	51.21	47.20	195.73	293.7
8.90	10.67	52.52	48.38	198.00	299.9
9.43	11.15	53.83	49.55	200.18	305.1

Table 1 (*Continued*)

T (K)	C_p° (J/(K mol))	T (K)	C_p° (J/(K mol))	T (K)	C_p° (J/(K mol))
202.44	310.0	289.77	512.0	241.12	409.8
204.69	314.6	291.60	516.8	243.32	415.4
206.93	321.8	293.50	521.1	245.52	423.1
209.18	327.4	295.30	525.8	247.69	427.3
211.42	332.1	297.10	529.2	249.86	435.5
213.66	338.8	298.60	532.3	252.00	444.9
215.89	344.2	300.35	538.9	254.16	455.3
218.11	350.6	302.11	544.4	256.31	467.2
220.33	355.3	303.83	549.5	260.39	515.2
222.52	361.4	305.53	551.2	262.49	547.1
224.73	364.9	307.15	556.8	264.58	571.1
226.90	369.7	308.83	560.3	266.68	561.8
229.09	375.7	310.48	565.9	268.80	532.2
231.26	383.1	312.13	567.0	273.00	491.5
235.45	394.0	313.75	570.2	275.07	486.6
237.58	400.2	315.36	575.8	277.12	487.1
241.85	411.9	316.96	577.1	279.16	491.2
243.98	415.4	318.54	581.1	281.18	493.2
246.10	424.7	320.10	587.1	283.19	497.0
248.21	431.6	321.66	588.3	285.20	501.8
250.31	437.0	323.19	591.4	287.19	506.8
252.37	447.1	324.19	593.8	289.18	510.3
254.45	456.4	325.69	598.4	291.14	516.1
256.52	470.2	327.19	599.6	292.78	521.5
258.57	488.6	328.66	603.0	294.74	526.7
260.61	517.4	330.12	608.7	296.63	529.2
262.64	549.3	331.56	610.7	298.55	532.6
264.67	571.2	332.90	613.4	300.47	537.1
266.70	562.1	334.32	616.2	302.35	542.3
268.47	532.0	335.71	619.2	304.20	548.2
270.51	509.2	337.09	622.2	306.03	551.2
272.48	494.8	338.45	625.2	307.85	556.9
274.44	488.1	Series 5		309.60	557.5
276.41	487.2	225.57	370.3	311.39	561.2
278.37	487.9	227.71	373.9	313.16	567.2
280.31	494.1	229.96	381.5	314.86	573.2
282.24	496.7	232.21	386.8	316.61	575.4
284.16	502.4	234.45	392.2	318.36	579.2
286.06	504.0	236.68	397.9	320.07	582.4
287.90	509.0	238.91	402.5		

the apparent heat capacities BDEB and BCE′B in the transition range, the enthalpy of transition in the sample under study is some times smaller than that of C_{60}. As shown in [26–28], the transformation of fullerite C_{60} is related to the phase transition of an orientation-ordered simple cubic phase of C_{60} to an orientation-disordered face-centered cubic phase where the C_{60} molecules make a virtually free rotation. This phase transition is reversible. The temperature corresponding to the maximum value of the apparent heat capacity in the transition range 185–280 K ($C^\circ_{p,\max} = 571.2$ J/(K mol)) is regarded as transition temperature for DS, $T^\circ_{\mathrm{tr}} = 264.7$ K. The enthalpy of transition, $\Delta_{\mathrm{tr}}H^\circ = 1.56 \pm 0.03$ kJ/mol, was determined graphically as the area bounded with BDEB curve (Fig. 1). According to [26], the corresponding values for C_{60} are the following: the transition temperature from 185 to 275 K, $T^\circ_{\mathrm{tr}} = 260.7$ K ($C^\circ_{p,\max} = 34747$ J/(K mol), $\Delta_{\mathrm{tr}}H^\circ = 7.46 \pm 0.15$ kJ/mol). It is suggested that the transformation, found in the

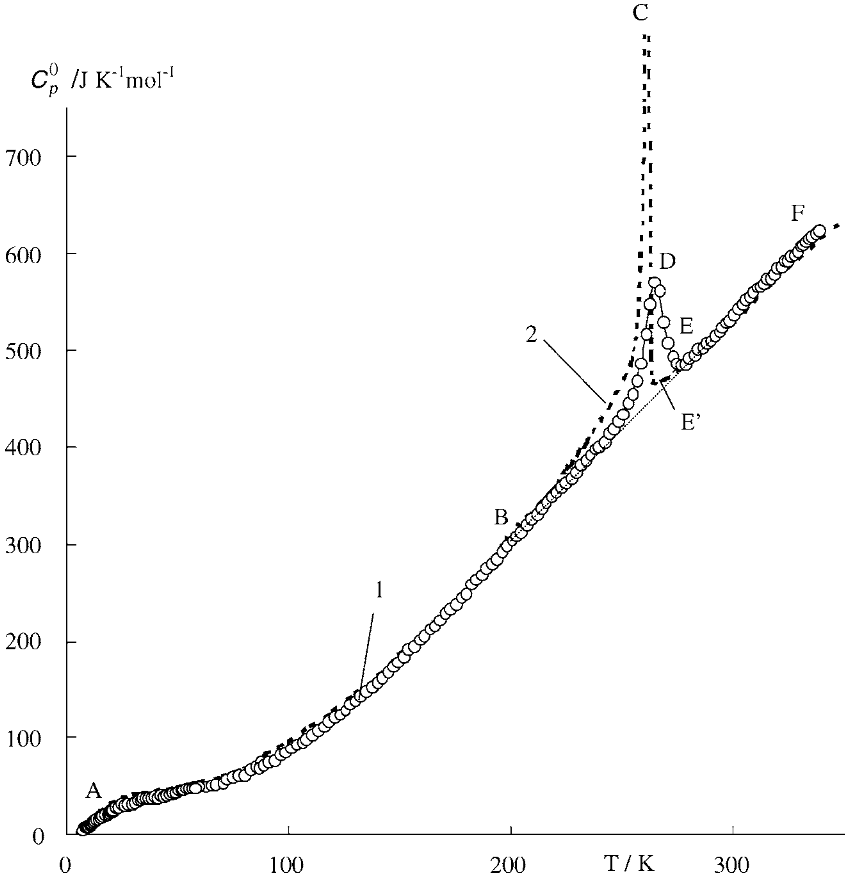

Fig. 1. Temperature dependence of heat capacity of: (1) DS sample; (2) the fullerite C_{60} [26].

DS sample, occurs because of the presence of C_{60} non-transformed to dimer $(C_{60})_2$. Based on that, the amount of residual C_{60} in the DS sample can be estimated by the expression:

$$n(C_{60}, \text{mol\%}) = \left[\frac{\Delta_{\text{tr}} H^\circ(\text{DS})}{\Delta_{\text{tr}} H^\circ(C_{60})}\right] \times 100\% \quad (1)$$

By substituting the proper numerical values into Eq. (1), the content of C_{60} in the sample of DS was determined to be 20.9 ± 0.9 mol%. This result coincides satisfactorily with the value determined from the spectral data (ca. 20 mol%). It is noted that the glass-like transformation (G-transition; [29]), observed for the initial C_{60} in the 81.0 to 88.5 K range ($T_G^\circ = 86$ K [26]), does not appear on the relation C_p° versus T. Meanwhile, a G-transition was observed in the DS sample in the range of 46–56 K ($T_G^\circ = 50$ K). It is far lower than in the case of C_{60}. The glass-like transition seems to be associated also with the freezing of hindered motions of $(C_{60})_2$ molecules in the crystalline lattice likewise to C_{60}.

The values of the normal heat capacity for the mixture of C_{60} and $(C_{60})_2$ in the DS sample in the transition interval were obtained by linear interpolation of the $C_p^\circ(T)$ curve from point B to point E (dotted line BE, Fig. 1). Curve ABDEF represents $C_p^\circ(T)$ for an additive mixture of 21 mol% C_{60} and 79 mol% the dimer $(C_{60})_2$.

Using the heat capacities of the mixture and fullerite C_{60}, the heat capacity of a pure dimer $(C_{60})_2$ was calculated per mole of C_{60} by:

$$0.79C_p^\circ\{(C_{60})_2\} + 0.21C_p^\circ(C_{60}) = C_p^\circ(\text{DS}) \quad (2)$$

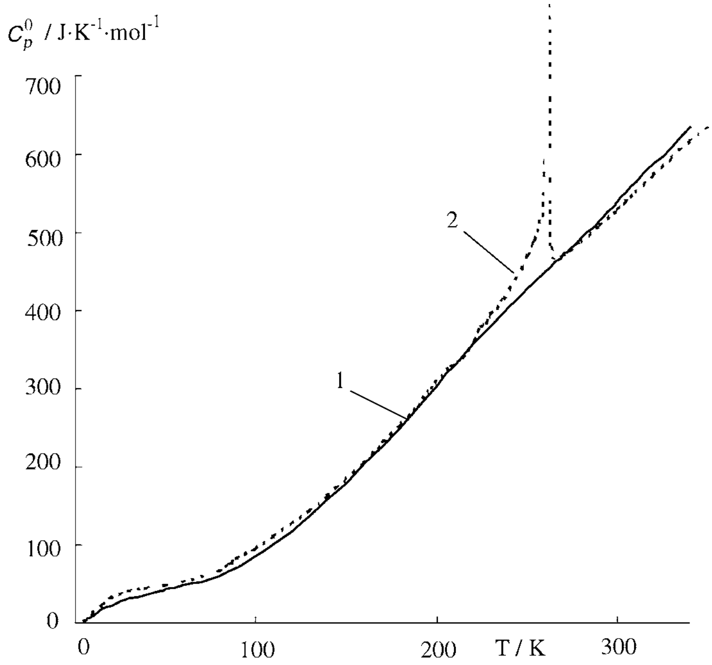

Fig. 2. Temperature dependence of heat capacity of: (1) the crystalline dimer $(C_{60})_2$ per mole of C_{60}; (2) the fullerite C_{60}.

where $C_p^\circ\{(C_{60})_2\}$, $C_p^\circ(C_{60})$ and C_p°(DS) denote the molar heat capacities of the fullerene dimer, fullerite and the mixture measured. The C_p° values for the dimer are given in section “thermodynamic functions”.

From these data, the relationship C_p° versus T for $(C_{60})_2$ was constructed (Fig. 2). The Figure illustrates for comparison $C_p^\circ(T)$ of C_{60} [26] and it is seen that $C_p^\circ(T)$ of the dimer is lower than that of C_{60} between $T \to 0$ and 150 K. The maximal difference (26%) occurs near 30 K. In the range 150–240 K, the C_p° values of both compounds are close and at $T > 275$ K the heat capacity for the dimer is greater than that of C_{60}.

It was of interest to evaluate the fractal dimension D for the crystalline dimer. In the fractal variant of the Debye’s heat capacity theory [20,21], D is an exponent at T in the heat capacity function. The significance of D values for solid bodies gives information on the heterodynamics of their structure. According to Tarasov’s theory of heat capacity of solids [30,31], the relation C_p° versus T is proportional to T^1 in the lower temperature range for chain-structured bodies, T^2 for solids with layer structure and it is proportional to T^3 in the case of spatial structure. The D values can be fractional and then the solids have mixed structures such as chain-layer, layer-spatial and other, as demonstrated in [20]. D can be estimated from the experimental C_p° data from the slope of the corresponding rectilinear sections of a $\ln C_V^\circ$ versus $\ln T$ plot. It follows from formula (2):

$$C_V = 3D(D+1)kN\gamma(D+1)\xi(D+1)\left(\frac{T}{\theta_{\max}}\right)^D \quad (3)$$

where N is the number of particles in a molecule, k the Boltzmann constant, $\gamma(D+1)$ γ-function, $\xi(D+1)$ the Riemannian ξ-function, $\theta_{\max}$ the characteristic temperature and D the fractal dimension that can be equal to 1–4 [21]. If in Eq. (3), $3D(D+1)kN\gamma(D+1)\xi(D+1)$ is denoted A, this expression can be written as follows:

$$C_V = A\left(\frac{T}{\theta_{\max}}\right)^D \quad (4)$$

Without a substantial uncertainty it may be accepted that $C_p^\circ = C_V$ at $T < 60$ K. From the $\ln C_p^\circ$ versus $\ln T$ plot, it is found that between 20 and 45 K $D =$

1, $\theta_{\max} = 128.7\,\mathrm{K}$ for the dimer, within 1%. With decreasing temperature, the values of D increase because of the enhancement of the interactions among molecules of $(C_{60})_2$ as in the case of other solids of any structure. At $T < 12\,\mathrm{K}$ the heat capacity C_p° of the dimer is described by Debye's function for heat capacity, $C_p^\circ \sim T^3$:

$$C_p^\circ = nD\left(\frac{\theta_D}{T}\right) \tag{5}$$

where D represents the Debye function, n and θ_D are adjustable parameters. With $n = 3$ and $\theta_D = 40.88\,\mathrm{K}$ Eq. (5) reproduces the experimental C_p° values in the range 7–12 K with the uncertainty close to ±0.8%.

At $T < 50\,\mathrm{K}$, the fractal dimension D for fullerite C_{60} amounts to 3 that agrees with the spatial structure and for the dimer $D = 1$ that is in agreement with the chain structure.

3.2. Glass-like transition in $(C_{60})_2$

Fig. 3 illustrates again the $C_p^\circ(T)$ curves of the crystalline fullerene dimer and the fullerite C_{60} near the glass-like transitions. The nature of the G-transitions was discussed in detail, for example in [29] and for fullerite C_{60} in [26,32]. The thermodynamic parameters of the transitions are listed in Table 2.

For the dimer the temperature interval where the G-transition takes place, the G-transition temperature T_G° and the maximum heat capacity are determined graphically, as for the fullerite C_{60} [26]. The configurational entropy S_{conf}° was estimated by the equation proposed in [33]:

$$S_{\mathrm{conf}}^\circ = \Delta C_p^\circ(T_G^\circ)\ln 1.29 \tag{6}$$

The configurational entropy is a part of the residual (zero) entropy of $(C_{60})_2$ at 0 K, $S^\circ(0)$. The latter is the sum of two components: S_{conf}° related to the freezing of the fullerene dimer structure on the G-transition and the entropy of mixing S_{mix}° of orientational molecule positions at their constant ratio at $T < T_G^\circ$, i.e.

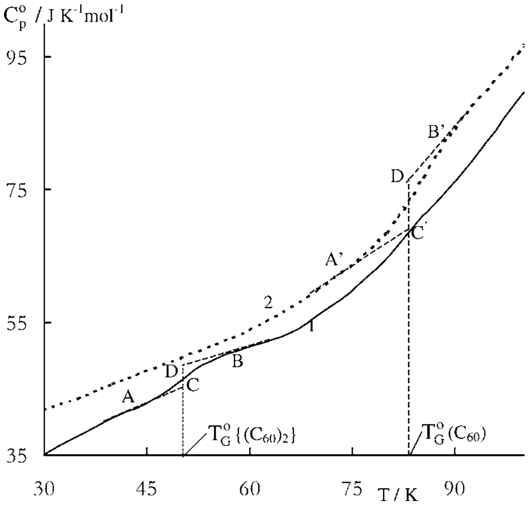

Fig. 3. Temperature dependence of heat capacity of: (1) the crystalline dimer $(C_{60})_2$ (per mole of C_{60}); (2) the fullerite C_{60} [26] with glass-like (G) transitions; AB and A′B′: temperature dependences of heat capacity on G-transition at T_G°; $T_G^\circ\{(C_{60})_2\}$ and $T_G^\circ(C_{60})$: temperatures of G-transitions of the dimer $(C_{60})_2$ and the fullerite (C_{60}).

$$S^\circ(0) = S_{\mathrm{conf}}^\circ + S_{\mathrm{mix}}^\circ \tag{7}$$

The entropy of mixing can be calculated by expression (8) [34]:

$$S_{\mathrm{mix}}^\circ = -R(N_1 \ln N_1 + N_2 \ln N_2) \tag{8}$$

where R is the universal gas constant, N_1 and N_2 are the mole fractions of molecular orientations of $(C_{60})_2$ molecules in the nodes of the crystalline lattice of the dimer, as in the case of $C_{60,}$ being frozen at T_G°. Unfortunately, the values of N_1 and N_2 for $(C_{60})_2$ are unknown. If it is assumed that the ratio of the entropy of mixing and the configurational entropy for $(C_{60})_2$

Table 2
Thermodynamics characteristics of G-type glass-like transitions in dimer $(C_{60})_2$ and fullerite C_{60}

Substances	Temperature interval of transitions (K)	T_G° (K)	ΔC_p° (T_G°, J/(K mol))[a]	S_{conf}°[a] (J/(K mol))	$S^\circ(0)$[a] (J/(K mol))
$(C_{60})_2$	46–56	50.0 ± 0.5	3.2 ± 0.5	0.81 ± 0.23	(3.4) ± 0.51
C_{60}	81.0–88.5	86.0 ± 0.5	4.5 ± 0.5	1.15 ± 0.44	4.5 ± 0.62

[a] Per mole C_{60}.

is the same as for the fullerite C_{60} (3.2 [26]) the value ofS°_{mix} for $(C_{60})_2$ is 2.6 J/(K mol). Then the zero entropy of the fullerene dimer is found to be $S^{\circ}(0) = 3.4$ J/(K mol). This is only a rough approximation. It is noted that the value of $S^{\circ}(0)$ of the dimer is less than 1% of the value of $S^{\circ}(T) - S^{\circ}(0)$ at 298.15 K and, therefore, the $S^{\circ}(0)$ value will not attribute a noticeable error to the estimation of the entropy of dimerization of C_{60} and the standard entropy of formation of the dimer from graphite at 298.15 K.

3.3. *Thermodynamic functions*

From the $C_p^{\circ}(T)$ curve of crystalline $(C_{60})_2$ the thermodynamic functions were calculated in the range of $T \to 0$ to 340 K (Table 3). The enthalpy $H^{\circ}(T) - H^{\circ}(0)$ and entropy $S^{\circ}(T) - S^{\circ}(0)$ were calculated by numerical integration of the relations. The Gibbs function $G^{\circ}(T) - H^{\circ}(0)$ was calculated from the values of $H^{\circ}(T) - H^{\circ}(0)$ and $S^{\circ}(T) - S^{\circ}(0)$ at corresponding temperatures (as described earlier [35]).

Table 3
Calculated thermodynamic functions of dimer $(C_{60})_2$ per mole of C_{60} ($M = 720.66$ g/mol)

T (K)	$C_p^{\circ}(T)$ (J/(K mol))	$H^{\circ}(T) - H^{\circ}(0)$ (kJ/mol)	$S^{\circ}(T) - S^{\circ}(0)$ (J/(K mol))	$-[G^{\circ}(T) - H^{\circ}(0)]$ (kJ/mol)
5	3.261	0.0043	1.151	0.0015
10	11.94	0.0437	6.251	0.0188
15	18.74	0.1199	12.34	0.0653
20	24.87	0.2288	18.57	0.1430
25	29.32	0.3664	24.70	0.2510
30	33.15	0.5228	30.38	0.3890
35	36.32	0.6969	35.74	0.5540
40	39.03	0.8855	40.78	0.7460
45	41.47	1.087	45.52	0.9614
50	45.21	1.303	50.06	1.200
60	50.21	1.788	58.89	1.746
70	55.09	2.309	66.92	2.375
80	63.44	2.896	74.75	3.084
90	74.15	3.587	82.87	3.871
100	87.58	4.402	91.41	4.739
110	102.1	5.342	100.4	5.700
120	119.2	6.462	110.1	6.753
130	138.6	7.761	120.5	7.901
140	159.3	9.238	131.4	9.163
150	181.0	10.94	143.2	10.53
160	204.1	12.86	155.6	12.03
170	227.8	15.03	168.6	13.64
180	252.3	17.42	182.4	15.40
190	278.2	20.08	196.7	17.29
200	305.4	22.99	211.6	19.34
210	333.5	26.19	227.2	21.53
220	361.5	29.66	243.4	23.89
230	388.6	33.41	260.0	26.40
240	413.7	37.42	277.1	29.09
250	436.4	41.67	294.4	31.94
260	456.7	46.14	312.0	34.98
270	475.5	50.80	329.6	38.19
280	493.8	55.65	347.2	41.57
290	513.8	60.70	364.9	45.13
298.15	534.3	64.96	379.4	48.16
300	539.5	65.95	382.7	48.87
310	564.6	71.47	400.8	52.79
320	587.2	77.23	419.1	56.89
330	608.9	83.21	437.5	61.17
340	635.0	89.42	456.1	65.64

3.4. Entropy of dimerization reaction and standard entropy of formation of fullerene dimer at 298.15 K

The reaction of dimerization of the fullerite as well as its polymerization proceeds via the mechanism [2+2] cycloaddition between two in parallels orientated C=C—bonds of adjacent molecules of the fullerite. As described elsewhere [36,37], the reaction process proceeds with the formation of a four-membered cycle according to the scheme

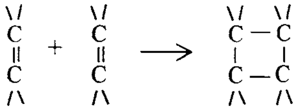

or

$$2C_{60}(\text{cr}) \rightarrow (C_{60})_2(\text{cr}) \qquad (9)$$

where (cr) is crystalline. According to Eq. (9), the entropy of reaction was determined to be $\Delta_r S^0 = -93.4\,\text{J/(K mol)}$. As expected, the entropy in process (9) decreases as it occurs almost in all reactions of association. The entropy value of the dimer was taken from Table 3 and that of the starting fullerite was given in [26].

The value of the standard entropy of formation of the fullerene dimer:

$$120C(\text{gr}) \rightarrow (C_{60})_2(\text{cr}) \qquad (10)$$

was calculated from the absolute entropies of graphite [38] and the fullerene dimer (Table 3, present work). This yields $\Delta_f S^\circ(C_{60})_2 = 71.6\,\text{J/(K mol)}$. The relatively small change of the entropy is, certainly, associated with the fact that both carbon in the form of graphite and the end product—the fullerene dimer—are rigid highly-ordered systems.

Acknowledgements

The authors wish to thank V.N. Agafonova and V.M. Senyavina for IR spectral analysis of the sample. The work was performed with the financial support of INTAS (project 00-807), the Russian Foundation of Basic Researches of RF (01-03-32061, 00-03-40136, 00-03-32600) and the Ministry of Science of RF (decision of 15 January 1996).

References

[1] S.J. Duclos, K. Brister, R. Haddon, A. Kortan, F. Thiel, Nature 351 (1991) 380.
[2] M. Nunnez-Requeiro, L. Marques, J.-L. Hodeau, O. Bethoux, M. Perroux, Phys. Rev. Lett. 74 (1995) 278.
[3] Y. Ywasa, T. Arima, R.M. Fleming, T. Siegrist, O. Zhou, R.C. Haddon, L.J. Rothberg, K.B. Lyons, H.L. Carter Jr., A.F. Hebard, R. Tycko, G. Dabbagh, J.J. Krajewsky, G.A. Thomas, T. Yagi, Science 264 (1994) 1570.
[4] I.O. Bashkin, V.I. Rashchupkin, A.F. Gurov, A.P. Moravsky, O.G. Rybchenko, N.P. Kobelev, Ya.M. Soifer, E.G. Ponyato, J. Phys.: Condens. Matter 6 (1994) 7491.
[5] V.D. Blank, et al., Phys. Lett. A188 (1994) 281.
[6] V.A. Davydov, L.S. Kashevarova, A.V. Rakhmanina, V.N. Agafonov, R. Seolin, H. Szwarc, Pis'ma Zh. Eksp. Teor. Fiz. 63 (1996) 778.
[7] V.V. Brazhkin, A.G. Lyapin, S.V. Popova, R.N. Voloshin, Yu.V. Antonov, S.G. Lyapin, Y. Kluev, A.M. Naletov, N.N. Melnik, Phys. Rev. B 56 (1997) 11465.
[8] V.D. Blank, S.G. Buga, G.A. Dubitsky, N.R. Serebryanaya, M.Yu. Popov, B. Sundqvist, Carbon 36 (1998) 319.
[9] V.A. Davydov, L.S. Kashevarova, A.V. Rakhmanina, V.M. Senyavin, R. Seolin, H. Szwarc, H. Allouchi, V. Agafonov, Phys. Rev. 61 (2000) 11937.
[10] T.L. Makarova, B. Sundqvist, R. Hohne, P. Esquinazu, Ya. Kopelevich, P. Scharff, V.A. Davydov, L.S. Kashevarova, A.V. Rakhmanina, Nature 413 (2001) 716.
[11] V.D. Blank, S.G. Buga, Nauka i zhizn 10 (1995) 61.
[12] V.V. Brazhkin, A.G. Lyapin, Usp. Fiz. Nauk 166 (1996) 893.
[13] V.D. Blank, et al., in: Proceedings of the Abstracts of Joint XV AIRAPT & XXXIII EHPRG International Conference on High Pressure Science & Technology, Warsaw, Poland, 11–15 September 1995, p 197.
[14] A. Dworkin, H. Szwarc, V.A. Davydov, L.S. Kashevarova, A.V. Rakhmanina, V. Agafonov, R. Ceolin, Carbon 35 (1997) 745.
[15] Y. Ywasa, K. Tanoue, T. Mitani, T. Yagi, Phys. Rev. B 58 (1998) 16374.
[16] B. Sundqvist, A. Fransson, A. Inaba, C. Meingast, P. Nagel, V. Pasler, B. Renker, T. Wagberg, in: Fullerenes: Recent Advances in the Chemistry and Physics of Fullerenes and Related Materials, vol. 6, 1998, p. 705.
[17] A. Inaba, T. Matsuo, A. Fransson, B. Sundqvist, J. Chem. Phys. 110 (1999) 12226.
[18] B.V. Lebedev, K.B. Zhogova, N.N. Smirnova, V.V. Brazhkin, A.G. Lyapin, Thermochim. Acta 364 (2000) 23.
[19] B.V. Lebedev, K.B. Zhogova, V.D. Blank, R.Kh. Bagramov, Izv. Akad. Nauk., Ser. chem. 2 (2000) 227.
[20] T.S. Yakubov, Docl. Akad. Nauk SSSR 310 (1990) 145.
[21] A.D. Izotov, O.V. Shebershneva, K.S. Gavrichev, in: Proceedings of the All Russian Conference on Thermal Analysis and Calorimetry, Kazan, 1996, p. 200.
[22] V.A. Davydov, L.S. Kashevarova, A.V. Rakhmanina, V.M. Senyavin, V. Agafonov, R. Ceolin, H. Szwarc, Pis'ma Zh. Eksp. Teor. Fiz. 68 (1998) 881.

[23] V.A. Davydov, L.S. Kashevarova, A.V. Rakhmanina, V.M. Senyavin, O.P. Pronina, N.N. Oleinikov, V. Agafonov, H. Szwarc, Pis'ma Zh. Eksp. Teor. Fiz. 72 (2000) 807.

[24] V.M. Malyshev, G.A. Milner, E.L. Sorkin, V.F. Shibakin, Prybory i Tekhnika Eksperimenta 6 (1985) 195.

[25] R.M. Varushchenko, A.I. Druzhinina, E.L. Sorkin, J. Chem. Thermodyn. 29 (1997) 623.

[26] B.V. Lebedev, K.B. Zhogova, T.A. Bykova, V.S. Kaverin, V.L. Karnatsevich, M.A. Lopatin, Izv. Akad. Nauk, Ser. Chem. 9 (1996) 2229.

[27] P.A. Heiney, J.E. Fisher, A.R. McChie, W.J. Romanow, A.M. Denenstein, J.P. McCauley Jr., A.B. Smith, D.E. Cox, Phys. Rev. Lett. 66 (1991) 2911.

[28] A. Dworkin, H. Szwarc, S. Leach, J.P. Hare, T.J.S. Dennis, H.W. Kroto, R. Taylor, D.R.M. Walton, C.R. Acad. Sci. Paris, Ser. II 312 (1991) 979.

[29] Yu. A. Pentin (Ed.), Physics and Chemistry of Solid State of Organic Compounds, Moscow, 1967.

[30] V.V. Tarasov, Zh. Fiz. Khimii 24 (1950) 111.

[31] V.V. Tarasov, G.A. Ynitsky, Zh. Fiz. Khimii 39 (1965) 2076.

[32] W.I.F. David, R.M. Ibberson, T.J.S. Dennis, J.P. Hare, K. Prassides, Europhys. Lett. 18 (3) (1992) 219.

[33] G. Adam, J.U. Gibbs, J. Chem. Phys. 43 (1965) 139.

[34] D.K. Stull, E.F. Westrum, G.R. Sinke, The Chemical Thermodynamics of Organic Compounds, Wiley, New York, 1969.

[35] B.V. Lebedev, Thermochim. Acta 297 (1997) 143.

[36] A.M. Rao, P. Zhou, K.A. Wang, G.T. Hager, J.M. Holden, Y. Wang, W.T. Lee, X.X. Be, P.S. Eklund, D.S. Cornett, M.A. Duncan, I.J. Amster, Science 259 (1993) 955.

[37] G.P. Karpacheva, Vysokomolek. Soed. 42 (2000) 1974.

[38] V.P. Glushko (Ed.), Thermodynamic Constants of Substances, No. 1, Part 1, VINITI, Moscow, 1965–1972.